Transfer Function Estimation of Telephone Lines from Input Impedance Measurements

Roberto M. Rodrigues, Claudomiro Sales, Aldebaro Klautau, *Senior Member, IEEE*, Klas Ericson, and João Costa, *Member, IEEE*

***Abstract*—The ability of a specific telephone line to support a certain digital subscriber line (DSL) service is determined by its downstream and upstream data rates, which are mainly dependent on the line's transfer function. In this way, methods for transfer function estimation play an important role on proper DSL deployment. Most of the existing methods derive the transfer function via line topology identification (LTI) processes. This paper proposes a method which directly estimates the transfer function of telephone lines without any previous LTI process. The results obtained from both simulations and experimental procedure using twisted-pair cables indicate that the proposed method achieves accurate estimations even for lines with bridged-taps.**

***Index Terms*—Digital subscriber line (DSL), impedance measurements, line qualification (LQ), single-ended line testing (SELT), transfer function estimation.**

I. Introduction

DIGITAL subscriber line (DSL) is a technology that enables broadband services over ordinary telephone lines in a cost-effective way. On the other hand, the legacy telephone network imposes challenges to the proper DSL deployment since it was designed to deliver the narrowband plain old telephone service (POTS). Therefore, it is important to assess whether the line under test (LUT) is capable of supporting DSL before service provisioning.

The term line qualification (LQ) identifies all the operator's tasks and related instruments used to assess the ability of a specific line to support a given DSL service. This ability is expressed by the downstream and upstream data rates, which are a function of the line's transfer function (attenuation) and noise level. By assuming conservative noise profiles, the LQ process can emit a judgment based on the estimation of the transfer function of the LUT [1], [2].

The transfer function depends on the line topology (total length, number of sections, employed cables, etc.) and, in principle, is estimated only by means of communication between equipments at the central office (CO) and the customer premises (CP), known as dual-ended line testing (DELT). This procedure provides the most accurate way for qualifying a line, but it necessarily requires dispatching a technician to the CP or a DSL service already deployed. Both cases prevent a cost-effective qualification before service provisioning.

Whenever DELT is not feasible or desirable, the transfer function can be indirectly estimated from the total line length or the full knowledge of the line topology.

Length-based qualification methods are based on the comparison between the line length and defined DSL deployment rules. The underlying idea is to associate the estimated length to an "average" attenuation, assuming a standard line topology. The length estimate can range from a plain radial distance from the serving CO via geographic information to precise determination from measurements performed from one end of the line, known as single-ended line testing (SELT). Unfortunately, length is not always an accurate data rate predictor since lines of the same length may have distinct topologies, and for consequence transfer functions [3].

Topology-based qualification methods estimate the transfer function from the full knowledge of the line topology, assuming a cable model. Therefore, line topology identification (LTI) is a mandatory intermediate step for this category of LQ methods. The identification of the line topology is based on the analysis of measurements on physical layer level [4], [5] and essentially exploits the fact that each line discontinuity[1] imposes a "signature" to the generated reflections. This allows to identify and characterize such discontinuities and, consequently, the line topology. Typically, topology-based methods perform better than length-based ones.

The qualification methods employing SELT presented in the literature rely on *a priori* knowledge of the LUT topology or perform LTI before actually estimating the transfer function [6]–[8]. Despite providing reasonably accurate results, several factors decrease the feasibility and effectiveness of such methods in practical situations.

1) In general, a combination of tools is used, such as: preprocessing [9], Bayesian networks [10], algorithm to determine the time of arrival of the reflections [4] and optimization [6]. This kind of sophisticated approach is difficult to be embedded in hardware with limited processing power;

Manuscript received October 19, 2010; revised April 6, 2011; accepted April 12, 2011. This work received financial support from the Research and Development Centre, Ericsson Telecomunicações S.A., Brazil. The Associate Editor coordinating the review process for this paper was Dr. Wendy Van Moer.

R. M. Rodrigues, C. Sales, A. Klautau, and J. Costa are with the Department of Electrical and Computer Engineering at the Federal University of Pará (UFPA), 66073-900 Belem-PA, Brazil (e-mail: menegues@ufpa.br; cssj@ufpa.br; aldebaro@ufpa.br; jweyl@ufpa.br).

K. Ericson is with the Broadband Technologies Laboratory/Department, 23 16480 Stockholm, Sweden (e-mail: klas.ericson@ericsson.com).

Color versions of one or more of the figures in this paper are available online at http://ieeexplore.ieee.org.

Digital Object Identifier 10.1109/TIM.2011.2157431

[1] A discontinuity is essentially an impedance mismatch on the line, such as: end of the line, a gauge change (i.e., two sections constitute this discontinuity), and a bridged-tap (i.e., three sections constitute this discontinuity).

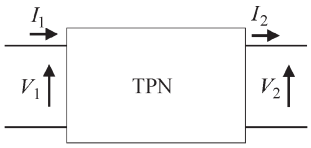

Fig. 1. General two-port network with indicated voltages and currents.

2) The LTI process is carried out via a comparison between measurements and theoretical counterparts generated from a cable model. Cable modeling concerns the design of parametric models for the primary or secondary parameters of twisted-pairs (e.g., the line sections) [11]–[13]. In spite of their importance, cable models may present a non-negligible mismatch from measurements since the real primary/secondary parameters may vary even from pair to pair of the same cable. This fact may easily mislead the identification process;
3) The length of the line sections is estimated assuming a mean value for the velocity of propagation (VoP). However, temperature, age, humidity and other factors can affect VoP [14]. Additionally, VoP is frequency dependent.

This paper proposes a method to estimate the transfer function of telephone lines without any previous topology identification process. Essentially, the proposed method employs a straightforward approach in which the overall ABCD parameters of the LUT are expressed only in terms of short and open-circuit input impedance measurements from the CO. Other methods for transfer function estimation from impedance measurements have been proposed in the literature. However, they estimate the line attenuation at only one specific frequency [15], use at least three impedance measurements [16] or need a previous length estimation process [17].

The remainder of this paper is organized as follows. Section II describes some concepts about two-port network (TPN) theory used in the proposed method, while Section III presents the proposed method. Section IV describes the evaluation process of the method as well as the achieved results. Section V presents the conclusions and future work.

II. Two-Port Network Concepts

A. Introduction

The underlying idea of TPN theory [18], [19] is to relate the terminal voltages and currents at the input port (V_1 and I_1) and the output port (V_2 and I_2) of a network to analyze it as a "black box". The currents and voltages are defined as shown in Fig. 1 and the variables that linearly relate them are called *parameters*–frequency-dependent ones.[2] Impedance (Z), admittance (Y) and transmission (T) or ABCD are examples of set of parameters [18].

Since each set of parameters relates the same signals,[3] a given set can be converted to another as showed in Table I,

TABLE I
Conversions Among Impedance, Admittance, and Transmission Parameters [21]

	Z		**Y**		**T**	
Z	z_{11}	z_{12}	$\frac{y_{22}}{det(\mathbf{Y})}$	$-\frac{y_{12}}{det(\mathbf{Y})}$	$\frac{A}{C}$	$\frac{det(\mathbf{T})}{C}$
	z_{21}	z_{22}	$-\frac{y_{21}}{det(\mathbf{Y})}$	$\frac{y_{11}}{det(\mathbf{Y})}$	$\frac{1}{C}$	$\frac{D}{C}$
Y	$\frac{z_{22}}{det(\mathbf{Z})}$	$-\frac{z_{12}}{det(\mathbf{Z})}$	y_{11}	y_{12}	$\frac{D}{B}$	$-\frac{det(\mathbf{T})}{B}$
	$-\frac{z_{21}}{det(\mathbf{Z})}$	$\frac{z_{11}}{det(\mathbf{Z})}$	y_{21}	y_{22}	$-\frac{1}{B}$	$\frac{A}{B}$
T	$\frac{z_{11}}{z_{21}}$	$\frac{det(\mathbf{Z})}{z_{21}}$	$-\frac{y_{22}}{y_{21}}$	$-\frac{1}{y_{21}}$	A	B
	$\frac{1}{z_{21}}$	$\frac{z_{22}}{z_{21}}$	$-\frac{det(\mathbf{Y})}{y_{21}}$	$-\frac{y_{11}}{y_{21}}$	C	D

which summarizes the conversions among impedance, admittance and transmission parameters.

The ABCD parameters relate the input to the output signals of a network as follows:

$$\begin{bmatrix} V_1 \\ I_1 \end{bmatrix} = \begin{bmatrix} A & B \\ C & D \end{bmatrix} \begin{bmatrix} V_2 \\ I_2 \end{bmatrix}. \tag{1}$$

B. ABCD Parameters Applied to Line Modeling

A telephone line connecting a user to a CO is usually made up of cable segments (line sections) in cascade, connected in series (serial section) or in shunt (bridged-tap). Ideally, each line section is assumed to be a uniform and homogeneous[4] transmission line.

The telegrapher's equations can be solved in such a way that it is possible to model each line section as a TPN. In this case, the ABCD parameters for each serial section are expressed by [23], [24]

$$\begin{bmatrix} V_1 \\ I_1 \end{bmatrix} = \begin{bmatrix} \cosh(\gamma l) & Z_0 \sinh(\gamma l) \\ \frac{1}{Z_0} \sinh(\gamma l) & \cosh(\gamma l) \end{bmatrix} \begin{bmatrix} V_2 \\ I_2 \end{bmatrix} \tag{2}$$

where l is the length, Z_0 is the characteristic impedance and γ is the propagation constant of the line. In a similar way, a bridged-tap can be modeled as

$$\begin{bmatrix} V_1 \\ I_1 \end{bmatrix} = \begin{bmatrix} 1 & 0 \\ \frac{\tanh(\gamma l)}{Z_0} & 1 \end{bmatrix} \begin{bmatrix} V_2 \\ I_2 \end{bmatrix}. \tag{3}$$

[2]For convenience, the frequency dependency of the currents and voltages as well as the parameters and quantities derived from them is omitted throughout this paper.

[3]Except scattering and transfer parameters [20] that relate incident and reflected signals of each port.

[4]The cross-section of a uniform line is longitudinally invariant throughout the entire length. A line is said homogeneous if the electrical and magnetic properties of the medium surrounding the conductors are the same everywhere [22].

Two other approaches can be employed to derive (2) and (3): from Caley–Hamilton theorem [25] and through image parameters [26].

This TPN modeling of the line sections is especially useful due to a property of the ABCD matrix called chain rule [27]. It states that: *for a given network made of several links, the overall ABCD matrix that characterizes the network will be the product of the ABCD matrices of each link*. In this way, the chain rule allows deriving the overall ABCD parameters of a line by the product of the ABCD modeling of each section.

From the overall ABCD parameters, any electrical characteristic of the LUT can be derived. Specifically, the transfer function of the line, defined as the ratio between V_2 and V_1, is calculated by [24]

$$H = \frac{V_2}{V_1} = \frac{Z_l}{AZ_l + B} \tag{4}$$

while the input impedance is calculated by

$$Z_{in} = \frac{AZ_l + B}{CZ_l + D}, \tag{5}$$

where Z_l is the load impedance connected to port 2.

C. Reciprocity and Symmetry

Reciprocity and symmetry are properties that essentially determine the number of parameters needed to completely characterize a certain TPN.

A TPN is reciprocal whenever it satisfies the reciprocity theorem [28], implying that the impedances z_{12} and z_{21} (or conversely the admittances y_{12} and y_{21}) are equal [19]. In other words, a reciprocal TPN means the signal transmission is the same regardless the direction of propagation. In terms of ABCD parameters, the determinant of the ABCD matrix is unitary, as can be noted in Table I. The general expression of the determinant of the ABCD matrix can be stated as

$$AD - BC = f_r \tag{6}$$

where f_r is a numeric value that determines the reciprocity level of the TPN, defined in this paper as *reciprocity factor*.

Symmetry can be better understood from another concept: image impedance. The image impedances associated to port 1 (Z_{I_1}) and port 2 (Z_{I_2}) of a TPN can be defined as two impedances, which when connected to the output and input of a network will induce the other impedance on the opposite port. In other words, an impedance with value Z_{I_1} terminating the TPN's port 1 implies an input impedance with value Z_{I_2} at TPN's port 2 and vice-versa [18], [29].

The image impedances do not depend on the loads connected to TPN's ports. They are properties of the network. Hence, Z_{I_1} and Z_{I_2} are defined only in terms of the parameters that characterize the TPN:

$$Z_{I_1} = \sqrt{\frac{AB}{CD}} \quad \text{or} \quad Z_{I_1} = \sqrt{\frac{z_{11}}{y_{11}}} \tag{7}$$

$$Z_{I_2} = \sqrt{\frac{DB}{AC}} \quad \text{or} \quad Z_{I_2} = \sqrt{\frac{z_{22}}{y_{22}}}. \tag{8}$$

Since z_{11} is the open-ended input impedance and $1/y_{11}$ is the short-ended input admittance, the image impedances of a TPN are commonly estimated by measuring, for each port, the open and short-ended input impedances and calculating their geometric mean [28].

The symmetry of a TPN can be defined as the square root of the ratio between its image impedances, i.e., [30]

$$f_s = \sqrt{\frac{Z_{I_1}}{Z_{I_2}}} \tag{9}$$

where f_s is a numeric value that determines the symmetry level between the TPN's ports and is defined in this paper as *symmetry factor*. A TPN is symmetric whenever its image impedances are equal, implying that $f_s = 1$. In other words, a symmetric TPN means symmetry with respect to the reflection at the ports.

Applying the left-hand definitions in (7) and (8) to (9), the symmetry factor can also be written as

$$f_s^2 = \frac{A}{D}. \tag{10}$$

This obviously implies that the parameters A and D are equal whenever the TPN is symmetric. Taking into account (10) and checking Table I, one can notice that symmetry is achieved whenever the input impedances z_{11} and z_{22} (or conversely the input admittances y_{11} and y_{22}) are equal [19].

Since the impedance and ABCD parameters are frequency-dependent quantities, both factors f_r and f_s are in essence frequency-dependent as well.

In summary, when a TPN is reciprocal or symmetric, only three parameters are needed to completely characterize it; when a TPN is reciprocal and symmetric, only two parameters are needed. Furthermore, the classical TPN theory also states that, even under reciprocity and symmetry conditions, the transmission parameters are expressed by: a) only DELT impedance measurements; or b) by a DELT and a SELT impedance measurements. This can be noticed by checking Table I. For example, the transmission parameter B for a certain TPN can be expressed in terms of impedance parameters as follows:

$$B = \frac{z_{11}z_{22} - z_{12}z_{21}}{z_{21}}. \tag{11}$$

If this TPN is reciprocal and symmetric, (11) is reduced to

$$B = \frac{z_{11}^2 - z_{12}^2}{z_{12}} \quad \text{or} \quad B = \frac{z_{22}^2 - z_{21}^2}{z_{21}}. \tag{12}$$

That is, at least one SELT impedance measurement (z_{11} or z_{22}) and one DELT impedance measurement (z_{12} or z_{21}) are needed to derive the parameter B from impedance parameters. The same holds for the other ABCD parameters, as can be noticed from Table I.

III. Proposed Method

A. Introduction

The most accurate LQ methods employing SELT model the sections of the LUT through (2) or (3), apply the chain

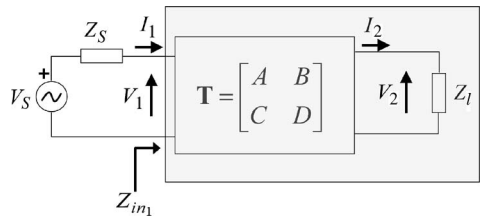

Fig. 2. Two-port network representation of a telephone line.

rule and, from the overall ABCD parameters, estimate the theoretical transfer function. In other words, these methods rely on knowing the line topology, or at least having an estimate. Furthermore, as presented in Section II-C, the classical TPN theory states that the overall ABCD parameters can only be expressed by SELT and DELT impedance measurements. In spite of that, this section will prove that both limitations can be overcome by simple mathematical manipulations to express the overall ABCD parameters that characterize a LUT only in terms of SELT impedance measurements from the CO.

B. General Description of the Method

The central idea of the proposed method is to analyze the line as a unique TPN, regardless of its topology. In this way, the network connecting the customer to the CO is modeled as depicted in Fig. 2: the voltage source V_s with internal impedance Z_s represents the measuring equipment located at the CO; the TPN represents the line itself; and the load impedance Z_l represents the line termination at CP.

For a certain frequency range $(f_{\min}, f_{\max})$, the input impedance of the line seen from the CO, Z_{in_1}, is expressed by (5). Whenever the CP is open ended (i.e., $Z_l = \infty$), (5) is reduced to

$$Z_{in_1}^{\infty} = \frac{A}{C}. \tag{13}$$

In the same way, whenever the CP is short circuited (i.e., $Z_l = 0$), (5) is reduced to

$$Z_{in_1}^{0} = \frac{B}{D}. \tag{14}$$

Applying (10) and (14) to the equation for the reciprocity factor, (6), yields

$$\frac{A^2}{f_s^2} - Z_{in_1}^{0}\frac{A}{f_s^2}C = f_r. \tag{15}$$

Now, if (13) is applied to (15), the parameter C can be expressed by

$$C = \sqrt{\frac{f_r f_s^2}{Z_{in_1}^{\infty}\left(Z_{in_1}^{\infty} - Z_{in_1}^{0}\right)}}. \tag{16}$$

Applying (16) to (13), the parameter A can be expressed by

$$A = \sqrt{\frac{f_r f_s^2 Z_{in_1}^{\infty}}{Z_{in_1}^{\infty} - Z_{in_1}^{0}}}. \tag{17}$$

If (17) is applied to (10), the parameter D will be expressed by

$$D = \sqrt{\frac{f_r Z_{in_1}^{\infty}}{f_s^2\left(Z_{in_1}^{\infty} - Z_{in_1}^{0}\right)}}. \tag{18}$$

Finally, applying (18) to (14), the parameter B can be expressed by

$$B = \sqrt{\frac{f_r Z_{in_1}^{\infty} {Z_{in_1}^{0}}^2}{f_s^2\left(Z_{in_1}^{\infty} - Z_{in_1}^{0}\right)}}. \tag{19}$$

Consequently, the transmission matrix $\mathbf{T}$ that characterizes the LUT as a whole is given by

$$\mathbf{T} = \begin{bmatrix} \sqrt{\frac{f_r f_s^2 Z_{in_1}^{\infty}}{Z_{in_1}^{\infty} - Z_{in_1}^{0}}} & \sqrt{\frac{f_r Z_{in_1}^{\infty} {Z_{in_1}^{0}}^2}{f_s^2\left(Z_{in_1}^{\infty} - Z_{in_1}^{0}\right)}} \\ \sqrt{\frac{f_r f_s^2}{Z_{in_1}^{\infty}\left(Z_{in_1}^{\infty} - Z_{in_1}^{0}\right)}} & \sqrt{\frac{f_r Z_{in_1}^{\infty}}{f_s^2\left(Z_{in_1}^{\infty} - Z_{in_1}^{0}\right)}} \end{bmatrix}. \tag{20}$$

The transfer function is then obtained by applying the estimated overall ABCD parameters to (4). Assuming impedance matching at high frequencies, the value used for the load impedance Z_l is the magnitude of the limit-value of the image impedance at the CO, i.e., $|Z_{I_1}(f = f_{\max})|$.

It is important to point out that (20) completely characterizes not only telephone lines but any network modeled as a TPN as well, and it does not restrict the analysis to any frequency band in special.

In [11], (Table IV, p. 7), the overall ABCD parameters of a TPN is presented, considering asymmetry of the line and hyperbolic functions. This derivation can be seen as a generalization of (2) for asymmetric lines. With some mathematical manipulations, one can derive the expression in [11] from (20) and vice-versa. Nevertheless, to the best of the authors' knowledge, the straightforward way of expressing the ABCD parameters of a TPN in (20) was never reported in the literature.

C. Discussion of the Method for Telephone Lines

1) Reciprocity Analysis: As described in Section II-B, each section of a line is assumed to be a uniform and homogeneous transmission line, and modeled by (2) or (3). One can notice that the determinants of both (2) and (3) are unitary, implying that any line section is ideally reciprocal. Moreover, it is well known that the determinant of a product of square matrices is equal to the product of the determinant of each square matrix, i.e.,

$$\det(\mathbf{T}_1 \times \mathbf{T}_2 \times \ldots) = \det(\mathbf{T}_1) \times \det(\mathbf{T}_2) \times \ldots \tag{21}$$

These properties indicate that a cascade of reciprocal line sections results in a reciprocal line. Therefore, any telephone line is ideally reciprocal $(f_r = 1)$, no matter its topology.

2) Symmetry Analysis: Unlike reciprocity, telephone lines in general do not obey the symmetry condition, even though each line section is assumed symmetric due to its presumable uniformity. For example, assuming a line made up of two (different) symmetric sections, where matrix $\mathbf{T}_1$ models the

first section (starting from the CO) and $\mathbf{T}_2$ models the second one, the overall ABCD matrix is given by

$$\mathbf{T}_1 \times \mathbf{T}_2 = \begin{bmatrix} a & b \\ c & a \end{bmatrix} \begin{bmatrix} x & y \\ z & x \end{bmatrix} = \begin{bmatrix} ax + bz & ay + bx \\ az + cx & ax + cy \end{bmatrix}. \quad (22)$$

By inspection of (22), it is clear that the overall parameter A $(ax + bz)$ is different from the overall parameter D $(ax + cy)$. This example shows that even a line with only two different sections can be asymmetric $(f_s \neq 1)$ [27].

In spite of telephone lines being typically reciprocal and asymmetric, one can notice from (20) that whenever symmetry is assumed, the overall ABCD parameters will be expressed only in terms of SELT input impedance measurements from the CO.

IV. Evaluation of the Proposed Method

A. General Conditions

The proposed method has been evaluated in three phases:

1) Baseline comparison: comparison with a state-of-the-art method using simulated data;
2) Evaluation using simulations: performance evaluation using simulated data for some European test lines [31];
3) Evaluation using measurements: performance evaluation using real cable measurements for some line topologies.

For phases one and two, the required measurements have been simulated based on the topologies of the test lines and the MAR# 2 cable model [11], [12]. Specifically: S_{11}^{∞} (open-ended one-port scattering parameter), $Z_{in_1}^{\infty}$, $Z_{in_1}^{0}$ and H were simulated in phase one while only $Z_{in_1}^{\infty}$, $Z_{in_1}^{0}$ and H were simulated in phase two. Fig. 3 depicts the simulation process for transfer function. For scattering and impedance quantities, the simulation process is the same except for the equation that derives the wanted quantity from the overall ABCD parameters—e.g., (5) is used to derive impedance. Additionally, no noise was inserted to the simulated data and the considered frequency range was the ADSL one: 256 tones, from 4.3125 kHz to 1.104 MHz. Regarding the load impedance for H calculation, the aim is to achieve the best impedance matching at the CP side, at high frequencies. As the MAR# 2 cable model provides a database for cables with characteristic impedance around 100 Ω, the load impedance was defined as 100 Ω.

For phase three, $Z_{in_1}^{\infty}$, $Z_{in_1}^{0}$ and H have been measured. The considered frequency range in the measurement process was the ADSL one. Each quantity was measured five times for each test line and its mean value used for the estimations. For transfer function measurements, the measuring instrument was an Agilent 4395A network analyzer while for input impedance measurements, the measuring instrument was an Agilent 4294A impedance analyzer. In both kind of measurements, 0301BB North Hills baluns (10 kHz–60 MHz, 50 Ω UNB—100 Ω BAL) were used for properly connecting the equipments and the twisted-pair cables.

In all three phases, the proposed method assumes the lines are reciprocal and symmetric, i.e., (20) with $f_r = 1$ and $f_s = 1$ is used to calculate the overall ABCD matrix of the LUT. The theoretical analysis presented in Section III-C2 indicated that

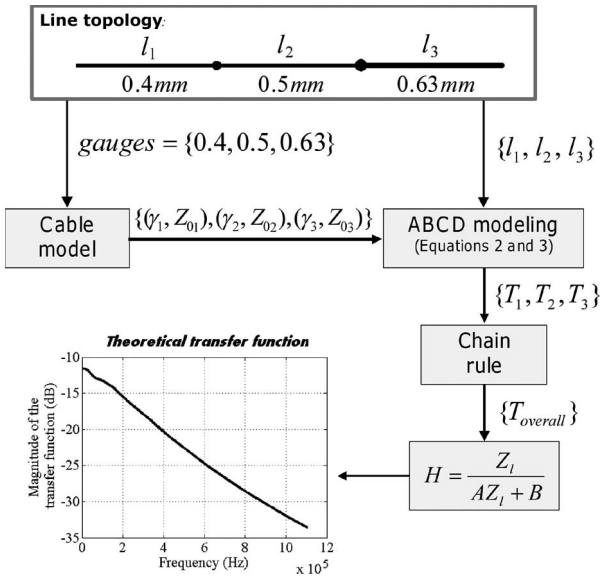

Fig. 3. Process employed to simulate the transfer function from a line topology. The process is illustrated considering a three-serial segments line as example.

only one-segment lines are symmetric. This means the majority of the line topologies in a telephone network can be considered asymmetric. However, to be asymmetric does not necessarily imply f_s to be much different than 1. A number of factors can determine an average asymmetry around 1. For example, even lines with a bridged-tap can be symmetric in case the sections after and before the tap are exactly the same (lengths and cable types). In other to quantify the reasonableness of the symmetry assumption with respect to the accuracy of the proposed method, a statistical analysis was performed. This analysis is reported in Appendix A and has indicated that, on average, the symmetry assumption results in reasonable estimations for typical lines.

The figure of merit used to evaluate the estimations is the magnitude of the deviation of the estimated transfer function $(\hat{H})$ with respect to the actual one (H), i.e.,

$$\left| 20 \log_{10} |\hat{H}| - 20 \log_{10} |H| \right| \text{ (dB)}. \quad (23)$$

The reason for adopting this figure of merit is twofold: the down/upstream data rates are determined from the magnitude of the transfer function and the noise profile [6]; there is a practical threshold for this figure of merit, defining that one bit is added/lost in each DSL tone in case the signal-to-noise ratio (SNR) is increased/decreased by 3 dB [32].

Fig. 4 provides a high-level illustration of the whole evaluation process carried out in all phases. It is important to notice that the simulated and measured transfer functions have been used only to evaluate the accuracy of the estimations provided by the proposed method and the chosen state-of-the-art one.

B. Baseline Comparison

This subsection presents a comparison between the proposed method and the state-of-the-art method described in [6]. For

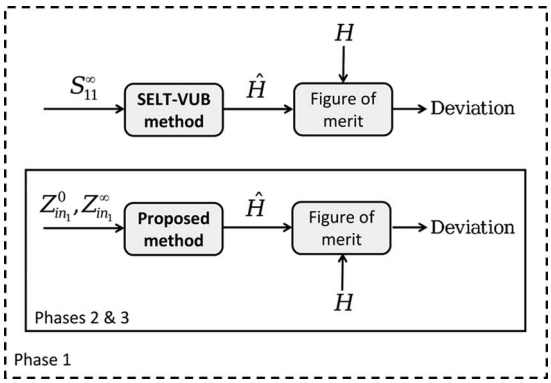

Fig. 4. Evaluation process for the three phases.

TABLE II
TOPOLOGY OF VUB LINES. "S" MEANS SERIAL SECTION WHILE "BT" MEANS BRIDGED-TAP. THE SEQUENCE OF LINE SECTIONS IS DISPOSED ASSUMING THE DIRECTION FROM THE CO (LEFT) TO THE CP (RIGHT)

		Topology	
Line	Type	Gauge (mm)	Length (km)
VUB # 1	s	0.5	0.9
VUB # 2	s - bt - s	0.5 - 0.5 - 0.5	0.9 - 0.2 - 0.7
VUB # 3	s - s	0.5 - 0.4	0.5 - 0.4

convenience, the latter is denoted as "SELT-VUB method" from now on. The goal here is to evaluate the performance of the proposed method taking as reference an accurate method.

The SELT-VUB method uses parametric models for both S_{11} and H quantities, based on three predefined topologies and VUB0 cable model [13]. A maximum likelihood estimation is carried out to estimate the parameters of the S_{11} model that best fits a given S_{11} measurement. The estimated parameters are then applied to H model to estimate the transfer function of the LUT. Summarizing, the method uses one SELT measurement, *a priori* knowledge of the line topology, optimization process and a cable model to estimate the transfer function. Three test lines were used in [6] to evaluate the method. They are described in Table II and are denoted here as "VUB lines".

For the current work, both the SELT-VUB method and associated VUB0 cable model were implemented strictly following the description in [6]. For the optimization process required by the method, the built-in Levenberg–Marquardt technique in MATLAB optimization toolbox was used and the initial guesses were calculated from the actual topologies of the VUB lines, as proposed in [6]. Even though the measurements are simulated and no noise is inserted, model errors appear on the estimations provided by the SELT-VUB method, since MAR #2 is used to simulate the measurements while the VUB0 cable model is used by the method. Anyhow, using the actual topology to calculate the initial guess is the best way to get as close as possible to the global minimum, even if this procedure is rarely feasible in practice. This makes the SELT-VUB method a performance reference to evaluate the proposed method.

The results obtained by the proposed and SELT-VUB methods are shown in Table III and Figs. 5–8. The estimations for

TABLE III
DEVIATION OF THE TRANSFER FUNCTION ESTIMATIONS—SELT-VUB METHOD VERSUS PROPOSED METHOD

	SELT-VUB method		Proposed method	
Line	Mean dev. (dB)	Max. dev. (dB)	Mean dev. (dB)	Max. dev. (dB)
VUB # 1	0.04	0.16	5.56×10^{-15}	3.90×10^{-14}
VUB # 2	0.09	0.30	0.04	0.35
VUB # 3	0.01	0.04	0.04	0.46

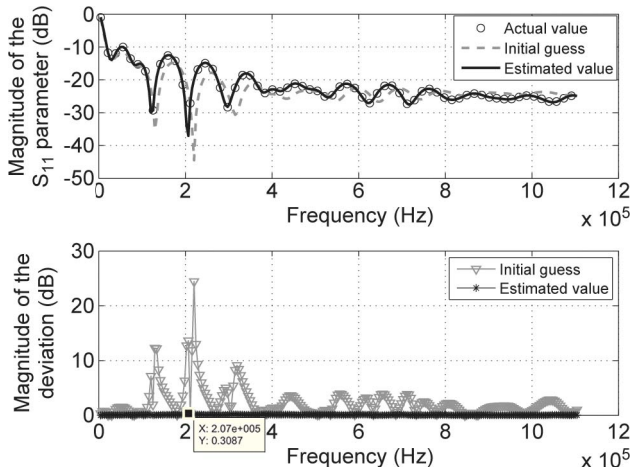

Fig. 5. (a) S_{11} simulated measurement and estimations and (b) deviations for VUB # 2.

both methods are accurate, with maximum deviations smaller than 0.5 dB for all test lines.

The SELT-VUB method achieved an accurate estimation of the parameters for all VUB lines. To illustrate that, Fig. 5 shows the S_{11} model for VUB # 2 line using the estimated parameters in comparison to the simulated measurement and the S_{11} model using the parameters provided by the initial guess. The estimated parameters provide a good match to the simulated measurement, providing a maximum deviation of 0.31 dB around 200 kHz. Similar performance was achieved for VUB # 1 and VUB # 3 lines. However, the SELT-VUB method performed comparatively better for the VUB # 3 line than for the other two lines. These results are unexpected since there are five parameters to be estimated for the VUB # 1 line while seven and ten must be estimated for VUB # 2 and VUB # 3, respectively [6]. This indicates that the optimization processes for the VUB # 1 and VUB # 2 lines potentially got stuck in local minima.

One point of concern about the SELT-VUB method is the configuration of the parameters of the optimization technique. From our experience using the method, this should be done individually, i. e., for each line under test, which is a problem in practical situations. Anyhow, the transfer function estimation provided by SELT-VUB was accurate and in accordance with the estimation of the parameters of the S11 model, as can be noted in Table III.

Regarding the proposed method, it provided an error-free estimation for VUB # 1 line, denoting the proposed ABCD modeling is correct. For VUB # 2 line, the obtained results were very similar to those provided by the SELT-VUB method

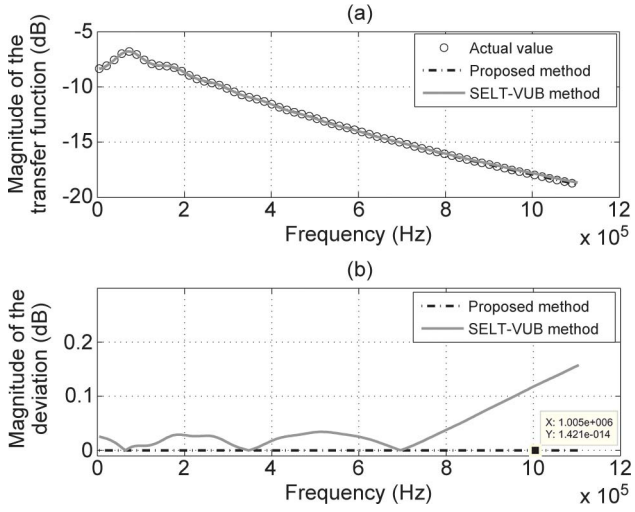

Fig. 6. (a) Transfer function estimations and (b) deviations for VUB # 1.

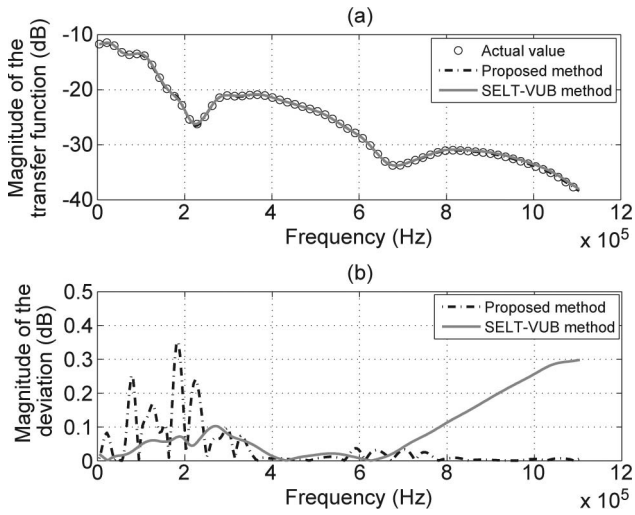

Fig. 7. (a) Transfer function estimations and (b) deviations for VUB # 2.

in spite of the line having a bridged-tap. This occurs because all line sections of VUB # 2 are of the same cable type and the difference in the lengths of the sections after and before the bridged-tap is only 200 m. In other words, VUB # 2 has an almost symmetric topology with respect to the bridged-tap (almost similar reflections at line's ports) and as a consequence a mean symmetry factor close to 1. Fig. 9 shows the symmetry factors for all VUB lines. The proposed method also performed well for VUB # 3 line, with maximum deviation less than 0.5 dB. However, the performance was comparatively worse than the one obtained with SELT-VUB. The reason is still the symmetry factor. VUB # 3 line is made of two different sections, yielding the highest mean symmetry factor among all VUB lines, as shown in Fig. 9.

It is possible to notice from the figures that the maximum deviations for the proposed method always occur at low frequencies. This is because, for asymmetric lines, the maximum amplitude of the symmetry factor occurs on that range, unlikely the employed assumption that the line is symmetric ($f_s = 1$ and frequency independent).

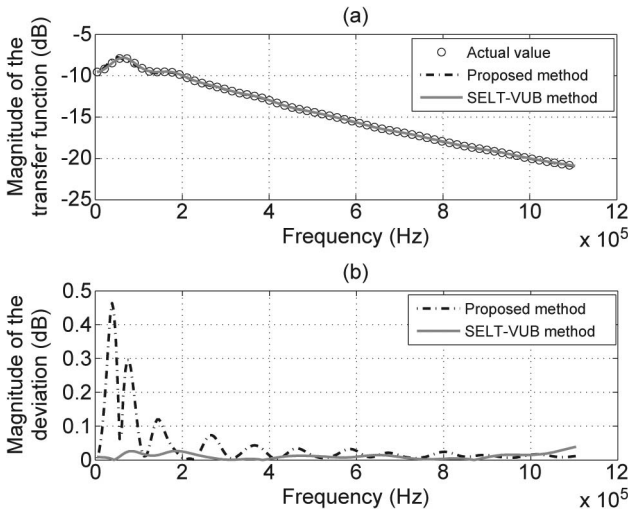

Fig. 8. (a) Transfer function estimations and (b) deviations for VUB # 3.

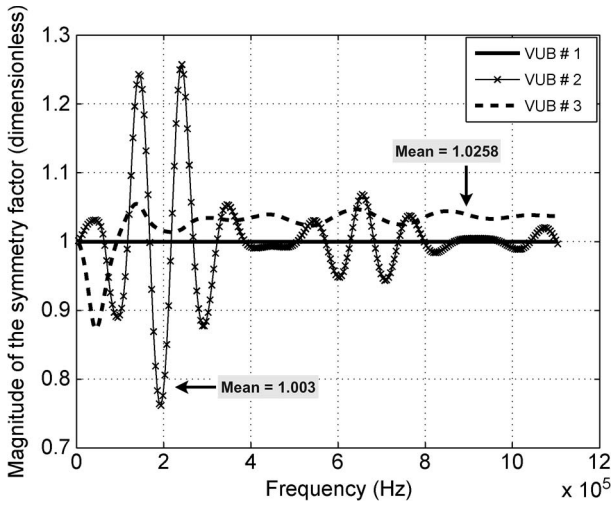

Fig. 9. Symmetry factor for VUB lines.

TABLE IV
TOPOLOGY OF ETSI LINES. "S" MEANS SERIAL SECTION WHILE "BT" MEANS BRIDGED-TAP. THE SEQUENCE OF LINE SECTIONS IS DISPOSED ASSUMING THE DIRECTION FROM THE CO (LEFT) TO THE CP (RIGHT)

	Topology		
Line	Type	Gauge (mm)	Length (km)
ETSI # 1	s	0.4	2.55
ETSI # 3	s - s	0.4 - 0.5	1.4 - 1.5
ETSI # 4	s - s - s - s	0.32 - 0.4 - 0.5 - 0.63	0.2 - 0.9 - 1.5 - 0.5
ETSI # 8	s - bt - s - bt	0.4 - 0.4 - 0.4 - 0.4	0.75 - 0.5 - 1.1 - 0.5

C. Evaluation From Simulated Data

For this phase, a set of test lines from the DSL recommendation [31] has been chosen. The considered European test lines were ETSI # 1, # 3, # 4, and # 8, with the adjustable length "x" set to give an overall insertion loss of 36 dB at 300 kHz. Their topologies are discriminated in Table IV.

Table V summarizes the results for ETSI lines while Figs. 10 and 11 show the estimations for ETSI # 4 and ETSI # 8, respectively. The results present a good match between the

TABLE V
DEVIATION OF THE ESTIMATIONS FOR ETSI LINES

Line	Mean dev. (dB)	Max. dev. (dB)
ETSI # 1	1.19×10^{-10}	1.61×10^{-9}
ETSI # 3	0.03	0.69
ETSI # 4	0.05	1.21
ETSI # 8	0.47	1.09

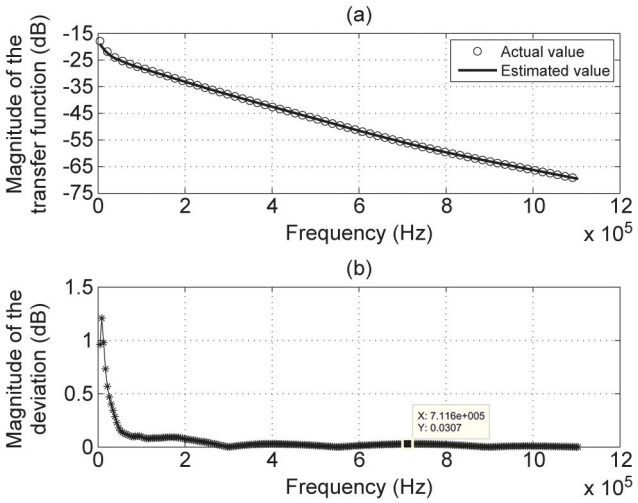

Fig. 10. (a) Transfer function estimation and (b) deviation for ETSI # 4.

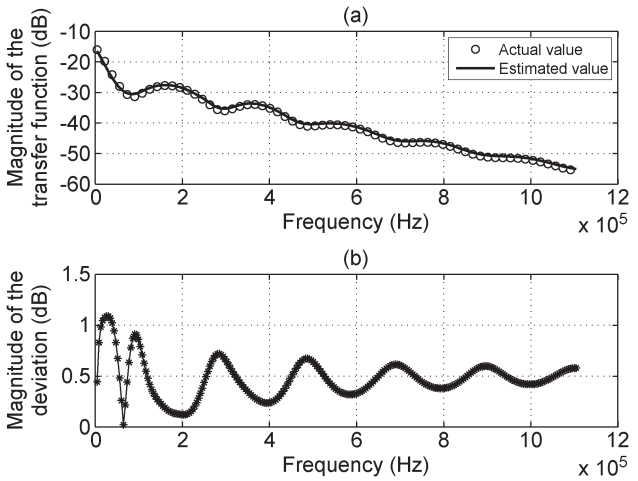

Fig. 11. (a) Transfer function estimation and (b) deviation for ETSI # 8.

estimated and the actual transfer function. In general, the estimations achieved maximum deviations smaller than 2 dB. As expected, it occurred at low frequencies. The best estimation is for ETSI # 1, with a negligible deviation, while the worst ones are for ETSI # 4 and ETSI # 8. This can be explained by the fact that ETSI # 1 is a single-section line, thus the symmetry assumption holds. On the other hand, ETSI # 4 is a four-section line, with four different gauges and lengths and ETSI # 8 is also a four-section line but with two bridged-taps, one of them close to CP. In this case, the bridged-tap close to CP causes a high asymmetry to the line, resulting in a bias on the symmetry factor

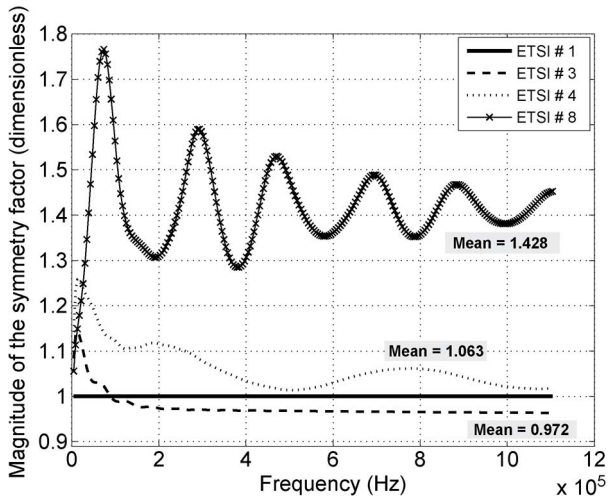

Fig. 12. Symmetry factor for ETSI lines.

TABLE VI
TOPOLOGY OF UFPA LINES. "S" MEANS SERIAL SECTION WHILE "BT" MEANS BRIDGED-TAP. THE SEQUENCE OF LINE SECTIONS IS DISPOSED ASSUMING THE DIRECTION FROM THE CO (LEFT) TO THE CP (RIGHT)

	Topology		
Line	Type	Gauge (mm)	Length (km)
UFPA # 1	s	0.4	1
UFPA # 2	s - s	0.4 - 0.5	0.5 - 1
UFPA # 3	s - s - s	0.4 - 0.5 - 0.4	0.2 - 1 - 0.5
UFPA # 4	s - bt - s	0.4 - 0.4 - 0.5	0.5 - 0.2 - 1
UFPA # 5	s - s - bt - s	0.4 - 0.5 - 0.4 - 0.5	0.2 - 0.5 - 0.5 - 0.5

and, consequently, on the deviation provided by the proposed method as well, as can be noted in Fig. 12.

From the results, it is possible to conclude that under ideal conditions (simulated data, without noise) the proposed method provides accurate estimations even for nonsymmetric lines.

D. Evaluation From Measured Data

For this final phase, five lines were defined. The criterion used to define their topologies was the cables available at our premises, (UFPA's DSL laboratory). They are discriminated in Table VI and called here "UFPA lines". UFPA lines were reproduced using two kinds of twisted-pair cables: Ericsson TEL 481 (0.4 mm/16 pairs) and Ericsson TEL 313 (0.5 mm/30 pairs).

Table VII presents the deviations for UFPA lines while Figs. 13–16 show the estimations for UFPA # 2, UFPA # 3, UFPA # 4 and UFPA # 5, respectively.

The estimated curves have presented a good match to the measured transfer functions, except for the first five tones (4.3125 to 17 kHz, approximately). The maximum deviation for all cases has occurred at the first tone, with values higher than 3 dB. To analyze these high deviations, it is important to note that, in this phase, there are two potential sources of error:

1) The lower cutoff frequency of baluns (10 kHz). This cutoff frequency causes an anomalous behavior of the

TABLE VII
DEVIATION OF THE ESTIMATIONS FOR UFPA LINES

Line	Mean dev. (dB)	Max. dev. (dB)
UFPA # 1	0.22	4.44
UFPA # 2	0.25	4.67
UFPA # 3	0.29	5.03
UFPA # 4	0.51	4.79
UFPA # 5	0.36	4.23

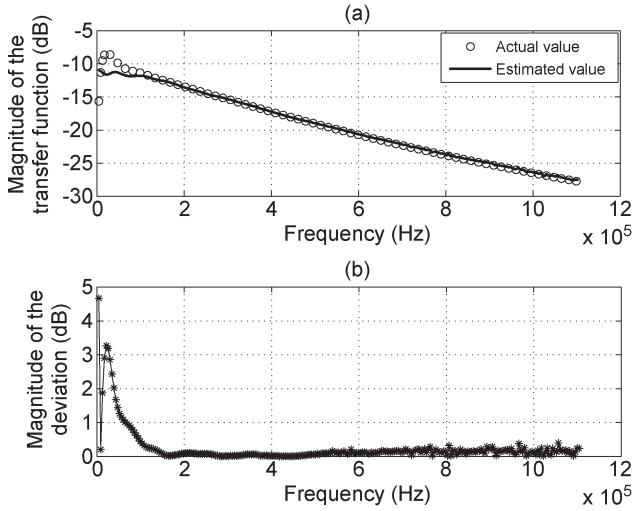

Fig. 13. (a) Transfer function estimation and (b) deviation for UFPA# 2.

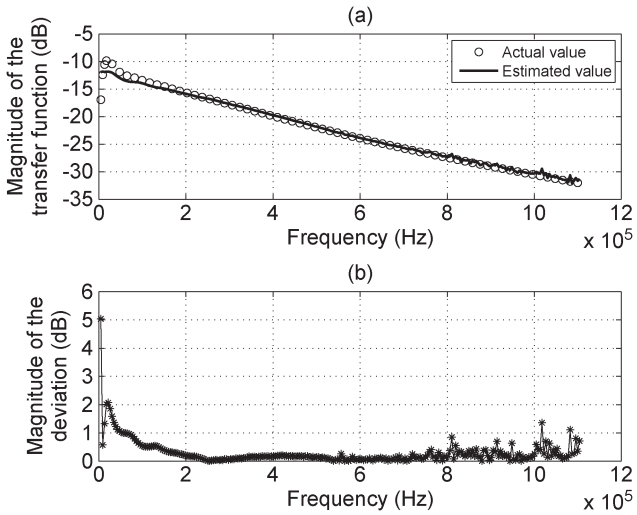

Fig. 14. (a) Transfer function estimation and (b) deviation for UFPA# 3.

measured transfer function at frequencies below and around it;

2) The symmetry assumption.

These sources of errors induce maximum deviations concentrated at the beginning of the frequency range and greater than desired. Moreover, this high-deviation biases the mean value.

In spite of that, the deviation for the remaining tones are low and, in a practical situation, the upstream (lower frequency range) used by the xDSL modems starts only at 25 kHz.

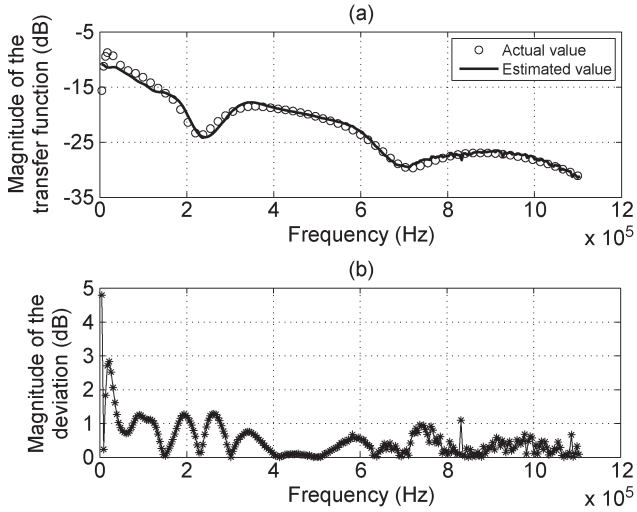

Fig. 15. (a) Transfer function estimation and (b) deviation for UFPA# 4.

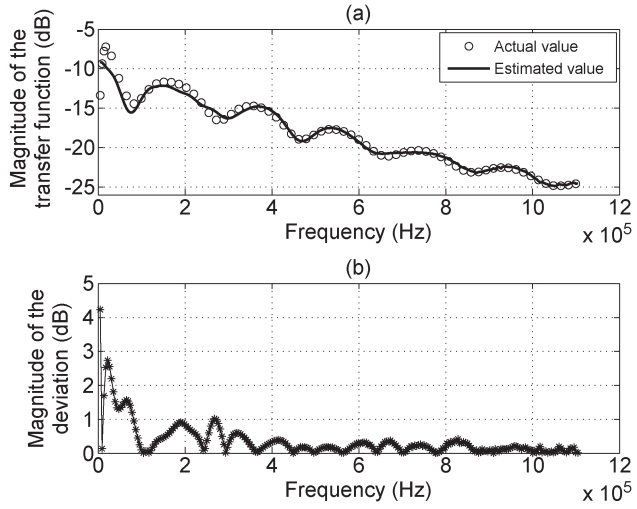

Fig. 16. (a) Transfer function estimation and (b) deviation for UFPA# 5.

V. CONCLUSION AND FUTURE WORK

In this paper, a method for transfer function estimation of telephone lines from one-port measurements is proposed. It avoids any previous line topology identification process and does not depend upon a cable model or *a priori* information about the LUT to estimate the transfer function. The method is based on a symmetry assumption that may not exactly hold in practical scenarios. However, this paper has shown that the accuracy of the estimations was reasonable for all considered test lines. Importantly, the method has a very low computational cost and employs a straightforward approach.

In general, the estimations provided by the proposed method presented very good match to the actual transfer function, even for lines with bridged-taps. Specifically, the proposed method provided mean and maximum deviations smaller than 0.5 and 1.21 dB, respectively, for simulated data. For measured data, the mean and maximum deviations were smaller than 0.6 and 5.1 dB, respectively.

It is known that an on-hook telephone set has a high impedance [20], [33]. Consequently, an open-ended input

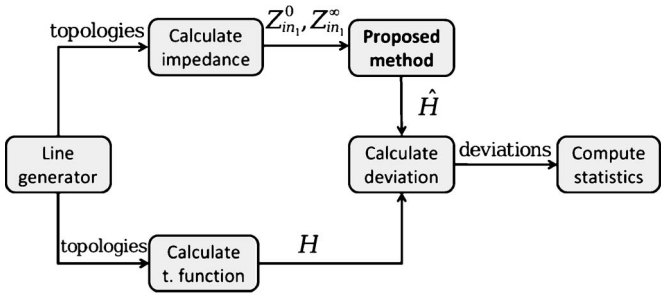

Fig. 17. Flowchart describing the employed statistical analysis.

impedance is feasible to be measured without human intervention at the CP side. On the other hand, there is no straightforward way to achieve a short at the remote site without human intervention. Even in case a short would be feasible by another telephone set state, e.g., off-hook, the telecom operator would still depend upon the end-user to set the required state. From the telecom operator's perspective, this is not desirable. Therefore, in practical situations, one drawback of the current version of the proposed method is the dependency of a short-ended input impedance measurement to estimate the transfer function from the CO. This fact lays the current version of the proposed method in between SELT and DELT-based methods. To properly adapt the proposed method to practical situations, a technique to estimate the short-ended input impedance without human intervention has been developed by our group. This technique is under development and will be the subject of another paper.

APPENDIX A
STATISTICAL ANALYSIS FOR THE SYMMETRY ASSUMPTION

This appendix presents a statistical analysis about the impact of the symmetry assumption over the estimation provided by the proposed method. The statistical analysis was carried out using simulation that randomly generated line topologies. Fig. 17 depicts the employed process.

The process starts with a line topology generator that feeds the next blocks with a large number of topologies. The line topology generator is a computational routine developed to randomly generate lines with parameters defined by the user.

For each generated topology, the input impedances $Z^\infty_{in_1}$ and $Z^0_{in_1}$, and the actual transfer function H are simulated over the considered frequency range. All three quantities are simulated from the same process, illustrated in Fig. 3. Following, the input impedances feed the proposed method that outputs the estimated transfer function $\hat{H}$. From the actual and estimated transfer functions, the deviation over frequency for each topology is calculated.

Ending the process, the generated data is used to create a 3-D histogram. This is done by dividing the deviation-frequency plane in a certain number of bins (sectors) and mapping the collection of points $(deviation(i), frequency(k))$, generated from all topologies, into the bins. This way, each bin has a certain number of occurrences, yielding a matrix of occurrences that is used to generate the 3-D histogram. This histogram provides a way to quantify the spreading of the points over the deviation-frequency plane.

TABLE VIII
FEATURES OF THE TEST CASES EMPLOYED IN THE STATISTICAL ANALYSIS

	Test-case	No. of sections	Total length range (km)	BT-length range (km)
Serial lines	a	2	[1, 3.5]	-x-
	b	3	[1.5, 3.5]	
	c	4	[2, 4]	
	d	5	[2.5, 4]	
Lines with BT(s)	e	3	[1.5, 3.5]	[0.2, 1]
	f	4	[2, 4]	
	g	5	[2.5, 4]	

The figure of merit used to evaluate the calculated deviations is again the 3-dB rule (23), that can be stated in its dimensionless form, i.e.,

$$0.779 < \left|\frac{\hat{H}}{H}\right| < 1.4125. \tag{24}$$

Additionally, the generated data is also used to calculate the percentage of lines with deviation great than 3 dB in at least one frequency sample.

A. General Simulation Conditions

The statistical analysis previously described was carried out for seven test cases. Table VIII summarizes the features of the line topologies generated for each test case. Test cases "a" to "d" regard the generation of lines with only serial sections while test cases "e" to "g" regard the generation of lines with one or more bridged-taps. Test cases "e" to "g" employ the following rules with respect to the generation of bridged-taps:

1) The first section never can be a bridged-tap;
2) Co-bridged-taps are not allowed;
3) A bridged-tap must be in between two serial sections or to be preceded by a serial section (whenever the last section is a bridged-tap);

Therefore: the generated lines in test case "e" can have only one bridged-tap, positioned on the second or the third section; the lines for test case "f" can have one or two bridged-taps from the second section on; and the lines for test case "g" can have up to three bridged-taps. For all cases, the available gauges used in the simulations are 0.32 mm, 0.4 mm, 0.5 mm, 0.63 mm, and 0.9 mm. The gauge sequence from central office to customer premises is always in ascending way, where the first gauge (0.32 mm) can be assigned only to the first line section while the last gauge can only be assigned to the last section. For bridged-taps, it is only possible to assign the same gauge of the previous serial section or the next thinner one.

Regarding the length of the generated lines, it was empirically defined a relationship between the number of line sections and the range of its total length. For example, for test case "b", all generated lines have total length ranging from 1.5 to 3.5 km. For lines with one or more bridged-taps, the defined total length

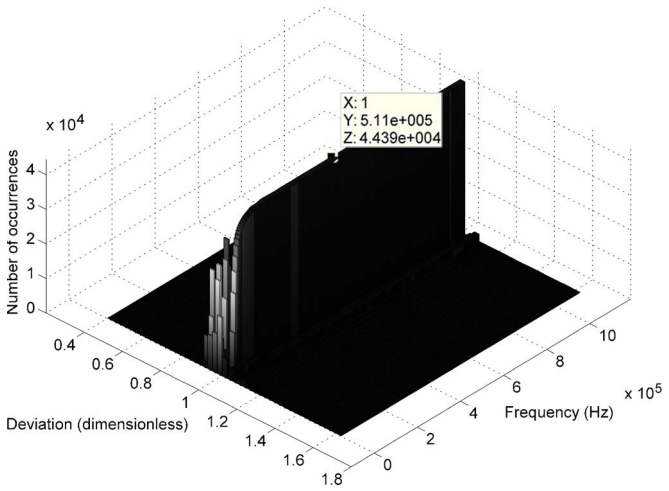

Fig. 18. Three-dimensional histogram for test case "a".

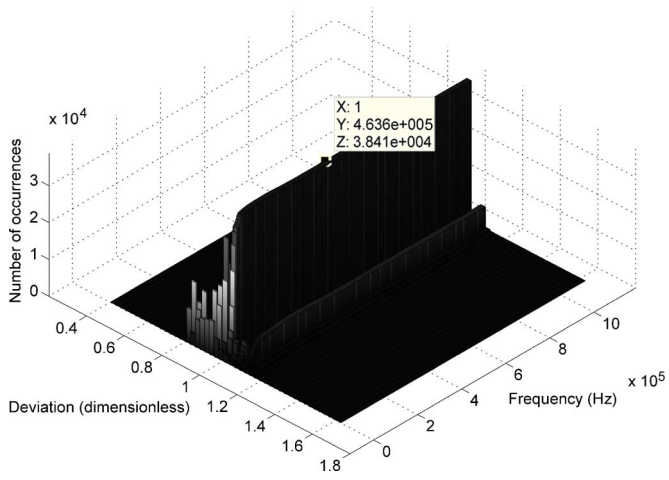

Fig. 19. Three-dimensional histogram for test case "d".

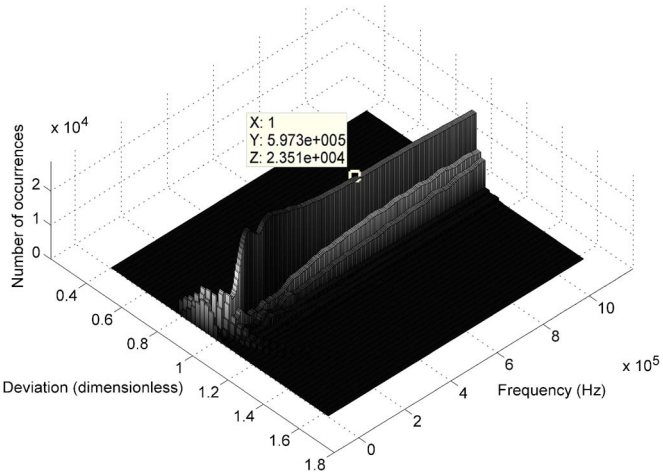

Fig. 20. Three-dimensional histogram for test case "e".

range regards to the main path connecting the CO and the CP sides (i.e., only the serial sections). The bridged-taps have their specific length range.

For each test case, 50 000 line topologies were generated. For the generation of the quantities of interest, the MAR#2 cable model is used and the considered frequency band corresponds to ADSL. Specifically about the generation of the actual transfer function, the load impedance used at the remote end of the lines is 100 Ω.

The proposed method estimates the transfer function of the generated topologies as described in the previous sections.

Regarding the statistics, the deviation axis is defined to range from 0.4 to 1.6 (dimensionless) and is divided in 49 bins. The frequency axis is defined to range from 4.3125 kHz to 1.104 MHz and is divided in 256 bins. This yields a matrix of occurrences with dimension 49 × 256. As each generated line provides 256 points, a total number of 12 800 000 points are mapped into the bins.

B. Results Analysis

The results for lines with only serial sections (test cases "a" to "d") have indicated that the presence of gauge changes alone does not result in a significant asymmetry of the line. Two of the histograms generated during the statistical analysis are presented in Figs. 18 and 19. These figures regard the histograms for test cases "a" (two serial sections) and "d" (five serial sections). In both, it is possible to see that the spreading of the points generated from the topologies are very concentrated around 1. Similar results were obtained for test cases "b" and "c". However, one can note that the spreading is relatively higher for low frequencies. This occurs because the asymmetry of the lines is in general more prominent at low frequencies since the image impedances have out-of-phase oscillations at that part of the frequency range—converging to a certain value at high frequencies.

Fig. 20 regards the histogram for test case "e" and gives a hint about the results obtained for lines with bridged-tap(s). In that figure, it is possible to note a much higher spreading of the points when compared to the cases with only serial sections. It is possible to see deviations around the 3-dB limit (1.4), mainly for low frequencies. Analyzing the results, it was noted that the topologies with a bridged-tap as the last section is the kind of line that provides the larger asymmetry.

TABLE IX
PERCENTAGE OF LINES WITH DEVIATION GREATER THAN 3 dB IN AT LEAST ONE DSL TONE, FOR EACH TEST CASE

	Test-case						
	a	**b**	**c**	**d**	**e**	**f**	**g**
p_{tone} (%)	0	0	0	0	0.716	2.86	5.824

Table IX summarizes the statistics collected for the analyzed test cases. The percentage of lines providing a deviation greater than 3 dB in at least one DSL tone was zero for test cases "a" to "d". For the test cases in which the topologies have one or more bridged-taps, the percentage can be considered small: less than 6%.

REFERENCES

[1] K. Kerpez, R. Faulkner, and P. Golden, "Evolving test and provisioning from POTS to xDSL services," in *Implementation and Applications of DSL Technology*. New York: Auerbach, 2007, ch. 5.

[2] J. R. i Riu, "Position paper on loop qualification and monitoring outlining general features the developed loop qualification and monitoring solution should fulfill," Ericsson AB, Stockholm, Sweden, Report IST-6thFP-507295, Nov. 2004.

[3] *DSL Anywhere—Issue 2*, Broadband Forum, Fremont, CA, Marketing Report MR-001. [Online]. Available: http://www.broadband-forum.org/marketing/marketingdocumentsarchive.php
[4] S. Galli and K. J. Kerpez, "Single-ended loop make-up identification-part I: A method of analyzing TDR measurements," *IEEE Trans. Instrum. Meas.*, vol. 55, no. 2, pp. 528–537, Apr. 2006.
[5] C. Sales, R. M. Rodrigues, F. Lindqvist, J. Costa, A. Klautau, K. Ericson, J. R. i Riu, and P. O. Börjesson, "Line topology identification using multi-objective evolutionary computation," *IEEE Trans. Instrum. Meas.*, vol. 59, no. 3, pp. 715–729, Mar. 2010.
[6] T. Bostoen, P. Boets, M. Zekri, L. Van Biesen, T. Pollet, and D. Rabijns, "Estimation of the transfer function of a subscriber loop by means of a one-port scattering parameter measurement at the central office," *IEEE J. Sel. Areas Commun.*, vol. 20, no. 5, pp. 936–948, Jun. 2002.
[7] K. J. Kerpez and S. Galli, "Single-ended loop-makeup identification-part II: Improved algorithms and performance results," *IEEE Trans. Instrum. Meas.*, vol. 55, no. 2, pp. 538–549, Apr. 2006.
[8] C. Neus, P. Boets, and L. Van Biesen, "Transfer function estimation of digital subscriber lines with single ended line testing," in *Proc. IEEE Instrum. Meas. Technol. Conf.*, May 2007, pp. 1–5.
[9] P. Boets, T. Bostoen, L. Van Biesen, and T. Pollet, "Preprocessing of signals for single-ended subscriber line testing," *IEEE Trans. Instrum. Meas.*, vol. 55, no. 5, pp. 1509–1518, Oct. 2006.
[10] T. Vermeiren, T. Bostoen, P. Boets, X. Ochoa Chebab, and F. Louage, "Subscriber loop topology classification by means of time-domain reflectometry," in *Proc. IEEE ICC*, May 2003, vol. 3, pp. 1998–2002.
[11] R. F. M. van den Brink, "Cable reference models for simulating metallic access networks," in *Proc. ETSI STC TM6*, 1998, pp. 1–40.
[12] J. Musson, "Maximum likelihood estimation of the primary parameters of twisted pair cables," in *Proc. ETSI STC TM6*, 1998, pp. 1–17.
[13] P. Boets, M. Zekri, L. Van Biesen, T. Bostoen, and T. Pollet, "On the identification of cables for metallic access networks," in *Proc. 18th IEEE IMTC*, May 2001, vol. 2, pp. 1348–1353.
[14] Riser Bond, Inc., *Introduction to Time Domain Reflectometers: Application Guide*. [Online]. Available: http://www.jw-ent.com/Images/Appguide.pdf
[15] K. Wong and T. Aboulnasr, "Single-ended loop characterization," *IEEE Trans. Circuits Syst. I, Fundam. Theory Appl.*, vol. 43, no. 12, pp. 996–998, Dec. 1996.
[16] D. Sabolic, A. Bazant, and R. Malaric, "Signal propagation modeling in power-line communication networks," *IEEE Trans. Power Del.*, vol. 20, no. 4, pp. 2429–2436, Oct. 2005.
[17] A. F. Jesen, F. Lindqvist, and A. Wia, "Method and arrangement for estimation of line properties," Patent WO 2004/099711 A1, Nov. 18, 2004.
[18] H. H. Skilling, "Two-port networks," in *Electric Networks*. New York: Wiley, 1974, ch. 12.
[19] J. G. Hong and M. J. Lancaster, "Network analysis," in *Microstrip Filters for RF/Microwave Applications,* 1st ed. New York: Wiley-Interscience, 2001, ch. 2.
[20] P. Golden, H. Dedieu, and K. Jacobsen, *Fundamentals of DSL Technology*. New York: Auerbach, 2006.
[21] D. M. Pozar, "The transmission (ABCD) matrix," in *Microwave Engineering,* 2nd ed. New York: Wiley, 1998, ch. 4.4.
[22] B. S. Guru and H. R. Hiziroglu, "A parallel-plate transmission line," in *Electromagnetic Field Theory Fundamentals*. Cambridge, U.K.: Cambridge Univ. Press, 2004, ch. 9.2.
[23] J. J. Werner, "The HDSL environment," *IEEE J. Sel. Areas Commun.*, vol. 9, no. 6, pp. 785–800, Aug. 1991.
[24] W. Y. Chen, "Twisted-pair channel modeling," in *DSL: Simulation Techniques and Standards Development for Digital Subscriber Lines*: Alpel Publ., 1997, ch. 3.
[25] P. L. D. Peres, I. S. Bonatti, and A. Lopes, "Transmission line modeling: A circuit theory approach," *SIAM Rev.*, vol. 40, no. 2, pp. 347–352, 1998.
[26] P. L. D. Peres, C. R. de Souza, and I. S. Bonatti, "ABCD matrix: A unique tool for linear two-wire transmission line modeling," *Int. J. Elect. Eng. Educ.*, vol. 40, no. 3, pp. 220–229, 2003.
[27] S. Galli, "Exact conditions for the symmetry of a loop," *IEEE Commun. Lett.*, vol. 4, no. 10, pp. 307–309, Oct. 2000.
[28] F. E. Terman, "Network theory, filters, and equalizers–Part I," in *Proc. IRE*, Apr. 1943, vol. 31, pp. 164–175.
[29] M. Mazilu and K. Dholakia, "Optical impedance of metallic nanostructures," *Opt. Express*, vol. 14, no. 17, pp. 7709–7722, Aug. 2006.
[30] M. Tse, *Impedance Matching for High-Frequency Design Elective*, 2003. [Online]. Available: http://cktse.eie.polyu.edu.hk/eie403/impedancematching.pdf
[31] *Test Procedures for Digital Subscriber Line (DSL) Transceivers*, ITU-T recommendation G.996.1, Feb. 2001.
[32] J. Z. Wu and C. R. Teeple, "Evaluation criteria for ADSL analog front end," *Analog Appl. J.*, pp. 16–20, Fourth quarter, 2003, [Online]. Available: http://focus.ti.com/lit/an/slyt051/slyt051.pdf
[33] S. Galli and D. L. Waring, "Loop makeup identification via single ended testing: Beyond mere loop qualification," *IEEE J. Sel. Areas Commun.*, vol. 20, no. 5, pp. 923–935, Jun. 2002.

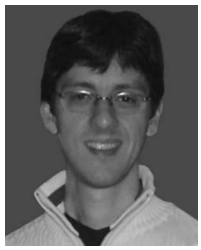

Roberto M. Rodrigues received the M.Sc. degree in electrical engineering from Federal University of Pará, Belém, Brazil, in 2005, where he is currently working toward the Ph.D. degree.

His main research interests are in the field of frequency domain identification of transmission lines, measurement systems, optimization techniques, and simulation systems.

Claudomiro Sales received the M.Sc. degree in electrical engineering from Federal University of Pará, Belém, Brazil, in 2005, where he is currently working toward the Ph.D. degree.

His major research interests are in the field of genetic algorithms, optimization techniques, measurements, and system identification. His current work is on loop identification using double-ended line testing for xDSL systems and multiobjective genetic algorithms.

Aldebaro Klautau (S'92–M'04–SM'08) received the Ph.D. degree from the University of California, San Diego, in 2003.

He was a faculty member of the Federal University of Santa Catarina, Florianopolis, Brazil, in 1995. He has been with the Federal University of Para (UFPA), Belem, Brazil, since 1996, where he is the Head of the Computer Engineering Department and affiliated to the Computer Science and Electrical Engineering graduate programs. He directs the Signal Processing and the Embedded Systems laboratories at UFPA. His research interests are in broadband communications, signal processing and machine learning.

Dr. Klautau is a researcher of the Brazilian National Council of Scientific and Technological Development.

Klas Ericson received the Ph.D. degree in applied electronics from Chalmers University of Technology, Gothenburg, Sweden, in 1984.

He has had various researcher and teaching positions within the area of medical engineering and general measurements and modeling as well as administrative positions as head of operation for some clinical engineering departments. His field of interest is measurements and modeling in an interdisciplinary setting, where he has published some original refereed scientific papers and has filed some patents.

João Costa (S'94–M'95) received the B.Sc. degree in electrical engineering from the Federal University of Pará, Belem, Brazil, in 1981, the M.Sc. degree in electrical engineering from the Pontifical Catholic University of Rio de Janeiro, Rio de Janeiro, Brazil, in 1989, and the Ph.D. degree in electrical engineering from the State University of Campinas, Campinas, Brazil, in 1994.

He is a Professor at the Federal University of Pará and a Researcher of the Brazilian Research Funding Agency. His research interests are toward the areas of electrical engineering, telecommunication, and computing.